Space Diversity Reception and Parallel Blind Equalization in Short-Burst TDMA Systems

Hongyi Qian, Tjeng Thiang Tjhung, *Senior Member, IEEE*, Ping He, and Fumiyuki Adachi, *Senior Member, IEEE*

***Abstract*—We consider a q-antenna space diversity system combined with two parallel equalizer branches for the reception of short-burst time-division multiple-access signals. By applying a combination of several recently proposed blind equalization algorithms, we make significant improvement over the burst error probability performance reported to date. This is achieved by starting the two blind equalizers from different initial tap settings and applying a specific weighting of the equalizers' outputs in order to derive the symbol decision. A burst error probability of less than 10^{-3} is achieved with the new strategy for a root mean square (rms) delay spread of less than 0.4 times the symbol duration. This is a significant improvement over a recently reported result.**

***Index Terms*—Blind equalization, burst error probability, parallel branches, short-burst time-division multiple-access (TDMA) system, space diversity reception.**

I. Introduction

In THIS paper, we consider the use of blind equalization in short-burst time-division multiple-access (TDMA) systems. In such systems, a frame contains a small number of bits (about 100). Usually, due to the fast time-varying nature of the channel, a training sequence has to be applied for each frame, leading to a very significant overhead. Therefore, the use of blind equalization is desirable. This problem has been considered recently by Chen *et al.* [1]. In [1], a blind T-spaced equalizer (T is symbol duration) with constant modulus algorithm (TSE-CMA) is applied on the same received burst repeatedly until convergence is achieved. However, it has been known that a single TSE suffers from local convergence and noise enhancement for channels with zeros near the unit circle [2]. Recently, some blind equalization algorithms have been proposed for use with a fractionally spaced equalizer and/or multiple antennas at the receiver, which can achieve global convergence under zero-forcing (ZF) conditions [4], [6]. In this paper, we consider a q-antenna space diversity receiver in which signal sampling is done at the baud rate $1/T$, as in [6] and [8], instead of a single TSE.

In [1], the burst error probability performance (a burst error occurs if a single burst has at least one bit in error) of the blind equalizer in a frequency-selective Rayleigh-fading channel is investigated, using simulation, as a function of the root mean square (rms) delay spread. Results have been obtained for the cases with two-branch space diversity and with reequalization. However, in [1], only a single TSE is used. Therefore, in [1], space diversity is not fully exploited and the receiver only achieves a burst error probability of 3×10^{-3} at an rms delay spread of 0.1 times the symbol duration. In this paper, we introduce a new strategy, to be explained in detail in a later section, that will improve the transmission performance quite significantly. The new strategy performs blind equalization in several parallel equalizer branches with different initial settings of the tap coefficients, where each equalizer makes use of the outputs from all the antennas. In addition, the final output is determined by weighting and combining the outputs of all blind equalizers in an appropriate and specific manner, to be described in Section III. We present simulation results in Section IV and offer conclusions in Section V.

Manuscript received February 21, 2001; revised June 18, 2001.

H. Qian is with the Semiconductor Product Sector, Motorola Electronics Pte. Ltd., Singapore (e-mail: Hongyi.Qian@motorola.com).

T. T. Tjhung and P. He are with the Center for Wireless Communications, National University of Singapore, 117674 Singapore (e-mail: tjhungtt@cwc.nus.edu.sg; heping@cwc.nus.edu.sg).

F. Adachi is with the Department of Electrical and Communication Engineering, Tohoku University, 980-8579 Sendai, Japan (e-mail: adachi@ecei.tohoku.ac.jp).

Publisher Item Identifier S 0018-9545(02)00436-X.

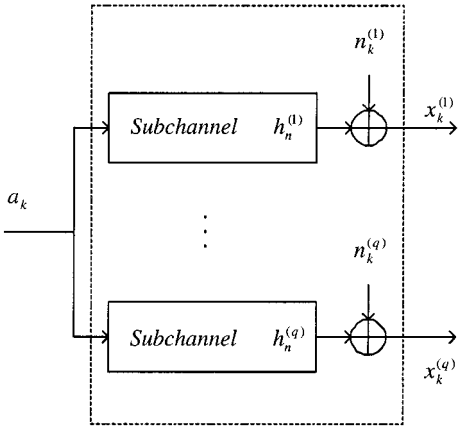

Fig. 1. Channel model of q-antenna space diversity system.

II. System Model

In this paper, we use an uncorrelated q-antenna diversity receiver, in which each antenna output is sampled at the baud rate $1/T$. The channel model is shown in Fig. 1. The propagation channel is considered to be a slow fading channel with discrete power-delay profile, where the delay between two adjacent paths is one symbol period. A typical channel power-delay profile is shown in Fig. 2. At the transmitter, the data shaping pulse $p(t)$ has a unit value in the interval $[0, T]$ and zero elsewhere. The receiver applies a matched filter with a square-pulse response $p'(t)$, which has value of $1/T$ in the interval $[0, T]$ and zero elsewhere. This response is realized by a one-symbol integrate-sample-and-dump filter. In general, the propagation

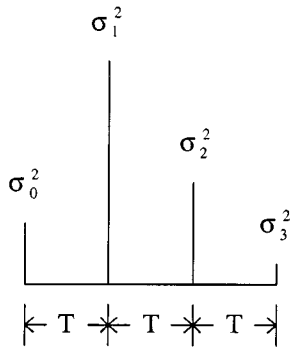

Fig. 2. A typical channel power-delay profile ($Q = 3$).

channel impulse response has a finite time duration. Therefore, the outputs of q subchannels become

$$x_k^{(i)} = \sqrt{E_s}\sum_{n=0}^{Q} a_{k-n}h_n^{(i)} + n_k^{(i)}, \qquad i = 1, 2, \ldots q \tag{1}$$

where

- $x_k^{(i)}$ sampled output of ith subchannel;
- a_n common transmitted sequence with differential quadrature phase-shift keying (DQPSK) modulation such that $|a_n| = 1$;
- $h_n^{(i)}$ sampled propagation channel impulse response of the ith subchannel;
- $n_k^{(i)}$ noise sample from additive white Gaussian noise with single-sided power spectrum density N_o;
- $Q+1$ number of multipaths;
- E_s symbol energy.

It is to be noted that the channel model in (1) is causal. That is, $h_n^{(i)}$ has nonzero value only when $0 \le n \le Q$. The derivation of (1) can be found in [9], by assuming a wide-sense stationary uncorrelated scattering slow fading channel with discrete power-delay profile and a matched filter detection of the signal.

In this paper, the subchannels are modeled as frequency-selective Rayleigh-fading channels that can be described as finite impulse response filters as in (1). $h_n^{(i)} = h_{n,r}^{(i)} + jh_{n,i}^{(i)}$ is a zero-mean complex Gaussian random variable, with $E[|h_{n,r}^{(i)}|^2] = E[|h_{n,i}^{(i)}|^2] = \sigma_n^2/2$, where $E[\cdot]$ denotes the ensemble average and σ_n^2 denotes the average power of the nth resolvable wave. Since the burst length is short, the channel impulse response can be considered as quasi-stationary, which means that for every burst, the channel does not change, but for a different burst, the channel is different. The rms delay spread is calculated as follows:

$$\tau_{\text{rms}} = \sqrt{\overline{\tau^2} - \bar{\tau}^2} \tag{2}$$

where $\bar{\tau} = \sum_n \tau_n\sigma_n^2, \overline{\tau^2} = \sum_n \tau_n^2\sigma_n^2, \tau_n$ is the delay of the nth path, and $\sum_n \sigma_n^2 = 1$ is assumed.

III. Blind Adaptive Equalization

In this paper, our parallel equalization strategy will employ two algorithms that are widely used for blind equalization: the mutually referenced (MR) equalization method [6] and Godard's algorithm [3] or constant modulus algorithm (CMA).

A. Mutually Referenced Equalization Method

It is known that blind equalization algorithms with a single TSE suffer from ill convergence [2]. Parallel equalization has been shown to be able to mitigate this problem [6]. In [6], a parallel blind equalization algorithm that exploits the property of MR second-order statistics has been proposed. In this algorithm, the output of every blind equalizer acts as a training sequence of other equalizers. To reduce the computation complexity, only two blind equalizers are used in this paper. The receiver with two parallel blind equalizers is shown in Fig. 3. The input of equalizer 1 is that of equalizer 0 delayed by one symbol period.

The structure of each blind equalizer is depicted in Fig. 4. One adjustable filter $\{c_{l,p}^{(i)}\}$ with length L is provided for each subsequence $\{x_k^{(i)}\}$. The output of each filter is

$$y_{l,k}^{(i)} = \sum_{p=0}^{L-1} x_{k-p-l}^{(i)}c_{l,p}^{(i)}, \qquad i = 1, 2, \ldots q \tag{3}$$

where $l = 0, 1$ denotes the lth blind equalizer. The output of the blind equalizer is

$$y_{l,k} = \sum_{i=1}^{q} y_{l,k}^{(i)}, \qquad l = 0, 1. \tag{4}$$

Since there are only two blind equalizers, the cost function of MR becomes

$$J_{\text{MR},l} = E[|y_{l,k} - y_{1-l,k}|^2]. \tag{5}$$

B. Constant Modulus Algorithm

In [7], it is mentioned that CMA will introduce random phase rotation. Therefore, we apply the modified CMA (MCMA) [1], [7], which can overcome this problem. The cost function of MCMA is

$$J_{\text{MCMA},l} = E\left[\left(y_{l,k,r}^2 - R_{r,2}\right)^2 + \left(y_{l,k,i}^2 - R_{i,2}\right)^2\right] \tag{6}$$

where

$$a_k = a_{k,r} + ja_{k,i} \tag{7}$$

$$y_{l,k} = y_{l,k,r} + jy_{l,k,i} \tag{8}$$

$$R_{r,2} = E\left(a_{k,r}^4\right)/E\left(a_{k,r}^2\right) \tag{9}$$

$$R_{i,2} = E\left(a_{k,i}^4\right)/E\left(a_{k,i}^2\right). \tag{10}$$

C. Combination of MR and MCMA

These two algorithms still suffer from ill convergence, although it has been proven in [4] and [6] that global convergence can be assured if ZF conditions, to be explained below, are satisfied. Let the transfer function of each subchannel be $H_i(z) = \sum_{n=0}^{Q} h_n^{(i)}z^{-n}$. Then the ZF conditions can be expressed as follows [4], [6].

1) There is no common zero for $\{H_i(z)\}_{i=1}^q$ (identifiability condition).
2) $L(q-1) \ge Q$ (equalizer length condition).

Since the ZF conditions cannot always be satisfied in a time-varying channel, these two algorithms, i.e., MR and MCMA, can be combined so that more information about the channel is used and better performance can be achieved. As in [5], we combine these two cost functions through a weighted constant α, such that

$$J_l = \alpha J_{\text{MCMA},l} + (1-\alpha)J_{\text{MR},l}. \tag{11}$$

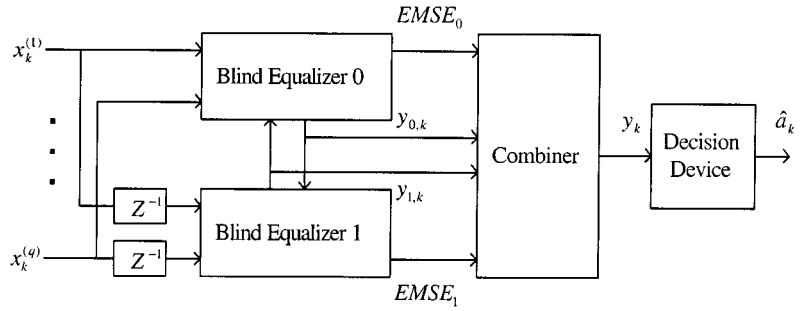

Fig. 3. Structure of a q-antenna diversity receiver with two blind equalizers.

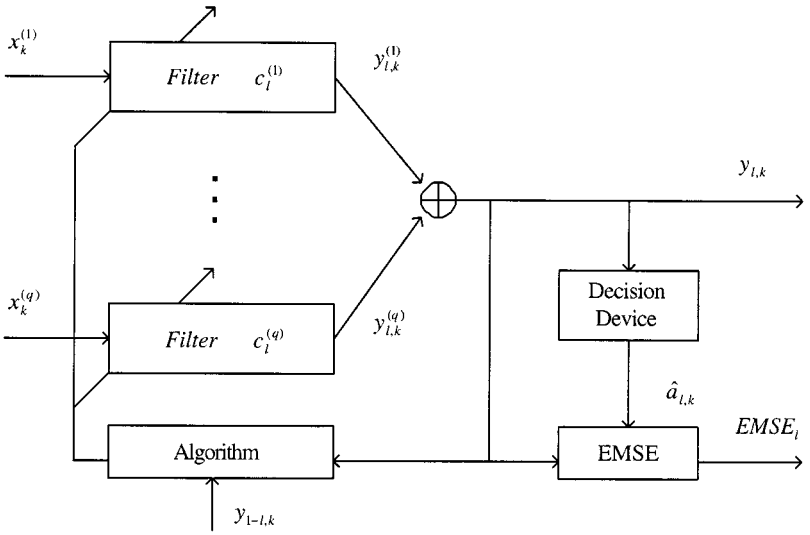

Fig. 4. Structure of individual blind equalizer.

It is proven in [8] that when the identifiability condition (lack of disparity) is not achievable, CMA still behaves quite robustly. On the other hand, the MR part of the cost function is sometimes able to prevent the new cost function from converging to local minima. By minimizing J_l with respect to the lth equalizer tap coefficients, the stochastic gradient descent algorithm can be formulated as follows:

$$\begin{aligned} c_{l,p}^{(i)}(m) - c_{l,p}^{(i)}(m+1) &= \Delta_l \left(x_{m-p-l}^{(i)}\right)^* \left[y_{l,m,r}\left(y_{l,m,r}^2 - R_{r,2}\right)\right. \\ &\quad \left. + jy_{l,m,i}\left(y_{l,m,i}^2 - R_{i,2}\right) + \gamma\left(y_{l,m} - y_{1-l,m}\right)\right] \end{aligned} \quad (12)$$

where $c_{l,p}^{(i)}(m)$ is the equalizer tap coefficient for the mth input symbol, Δ_l is a positive and small step size,* denotes conjugate, and $\gamma = (1-\alpha)/2\alpha$. The procedure for the derivation of (12) can be found in [10].

As described above, several parallel blind equalization strategies have been proposed and shown to be able to reduce ill convergence and improve the performance of a single blind equalizer [6]. One of our contributions in this paper is to apply different initial tap coefficient values to mitigate the ill convergence problem, as explained in the following. Different initial tap coefficient values correspond to different points on the surface of the cost function. Since there exist local minima for the cost function, if the initial estimated output is located near a local minimum, it will probably converge to the local minimum instead of the global minimum, which causes the wrong output. Moreover, for certain locations on the surface of the cost function, although global convergence can be achieved, the speed is slow. Hence, the output of the equalizer might not converge in a limited period.

Here, a parallel equalization strategy is used. Different initial tap coefficient values are assigned to several blind equalizers, which result in several estimated phase outputs. It is obvious that the most important factor for determining the shape of a cost function is the channel impulse response. Without having such information, it is very difficult to find starting points that can achieve global convergence. Therefore, random initial tap coefficient values are chosen for the parallel blind equalizers. The probability of all getting ill convergence or slow convergence becomes much smaller. After convergence, each equalizer will have an estimated mean square error (EMSE)

$$\text{EMSE}_l = \sum_{k=1}^{N} \frac{|y_{l,k} - \hat{a}_{l,k}|^2}{N} \quad (13)$$

where $\hat{a}_{l,k}$ is the output of the decision device of each blind equalizer, which is the estimation of a_k, and N is the frame size. EMSE_l is the value of EMSE calculated after every iteration.

Our other contribution in this paper is to choose the final output according to $y_k = \sum_l w_l y_{l,k}$, where w_l, the weightage associated with the lth blind equalizer, is given by

$$w_l = \frac{1/\text{EMSE}_l}{\sum_n (1/\text{EMSE}_n)}. \quad (14)$$

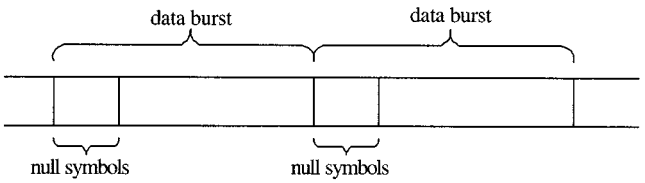

Fig. 5. Structure of data burst with null symbols.

The above choice of y_k ensures that output with small EMSE will be given a large weight. As a result, the probability of ill or slow convergence is reduced significantly.

Due to the ISI introduced by the causal channel, the received sequence is given by (1). As a consequence, the first few symbols of every received data burst will be affected by the unknown symbols in the previous data burst, which will degrade the error probability performance. Therefore, we use these symbols as null symbols where no signal is transmitted for these symbol periods so that the interference is reduced.

The structure of the data burst is shown in Fig. 5. Moreover, the drop in received power can be detected to find the beginning of a frame. The length of null symbols should be long enough so that the interference from the previous burst is removed or negligible. The null symbols are overhead, but we will show in Section IV that two to three null symbols are enough to remove interburst interference. The resultant overhead is still sufficiently small.

IV. Simulation Results

In this section, we demonstrate, through extensive computer simulations, the performance of the proposed algorithm for short-burst TDMA systems. A frame or burst of length $N = 60$ symbols (including null symbols) with DQPSK modulation is assumed for the transmission. When using QPSK, the output phase is shifted by unknown multiples of 90° from the input phase sequence. Due to this phase ambiguity, the DQPSK is used instead of QPSK, so that the detection will not be affected by the arbitrary phase rotation.

As mentioned before, the equalizer length conditions can be satisfied when $q = 2$ and $L \geq Q$. Therefore, each blind equalizer consists of two adjustable filters with length of $L = 5$, and two blind equalizers are used as mentioned before. Since MCMA is more robust than MR when ZF conditions are not satisfied, MCMA should be given more weight in the combined cost function. Hence, α is chosen to be 0.8 for all the simulations performed in this paper.

The channel input $\{a_k\}$ is an independent identically distributed sequence, and the channel noise is white Gaussian. The amplitude of the transmitted symbol is normalized to one. The step size is on the order of $10^{-3}/\sqrt{E_s}$, while its value is calculated according to the power of every received burst but is fixed during the iterations in order to achieve fast convergence. It is known that the convergence speed of blind equalization algorithm is slow; therefore, a long sequence of data is needed. For short-burst TDMA systems, in order to get convergence for each frame, the following iterative method is applied. The received sequence $x_k^{(i)}, k = 0, 1, \ldots N-1$, is extended according to $x_k^{(i)} = x_{k \bmod N}^{(i)}$ to form the input to the blind equalizer. It is equivalent to transmitting the same data burst through the same channel for a sufficiently long time so that convergence can be achieved at the receiver. Initial tap coefficient values are chosen randomly such that the coefficient with the maximum modulus is normalized to $1/\sqrt{E_s}$, and they vary according to the power of each received burst. Equalization will be stopped either when convergence is achieved, which is indicated by a small EMSE among all the equalizers, or when the number of iterations reaches a limit, which is 250 in our case. This is because one user cannot hold onto too long of a time in a TDMA system.

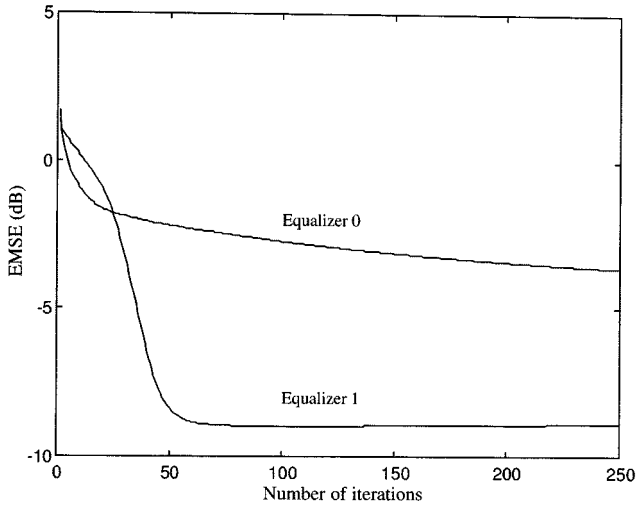

Fig. 6. Illustration of convergence behavior for parallel blind equalizers at $E_b/N_o = 20$ dB.

The MCMA-MR is first tested on a three-tap channel ($Q = 2$) for which the delay between two adjacent paths is one symbol period. Two null symbols are provided for every data burst. Perfect time synchronization is assumed in all cases. Fig. 6 illustrates a typical convergence behavior of equalizer outputs in a three-tap channel with $E_b/N_o = 20$ dB, where $E_b = E_s/2$ for DQPSK modulation and the sampled channel impulse response is given by

$$\begin{aligned}\left\{h_n^{(1)}\right\} &= \{0.338\,153 - 0.360\,157j, -0.373\,43 \\ &\quad + 0.112\,086j, 0.183\,196 + 0.012\,301j\} \\ \left\{h_n^{(2)}\right\} &= \{-0.550\,076 - 0.259\,515j, -0.498\,946 \\ &\quad + 0.677\,252j, -0.179\,217 + 0.115\,672j\}.\end{aligned}$$

The initial tap coefficient values for both equalizers are

$$\begin{aligned}\left\{c_{0,p}^{(1)}\right\} &= \{2, 0, 0, 0, 0\} \\ \left\{c_{0,p}^{(2)}\right\} &= \{0, 0, 0, 0, 0\} \\ \left\{c_{1,p}^{(1)}\right\} &= \{0, 1, 0.5, 0, 0\}\end{aligned}$$

and

$$\left\{c_{1,p}^{(2)}\right\} = \{0, 0, 0, 0, 0\}.$$

It can be seen that equalizer 1 is able to converge and give correct output although equalizer 0 does not converge.

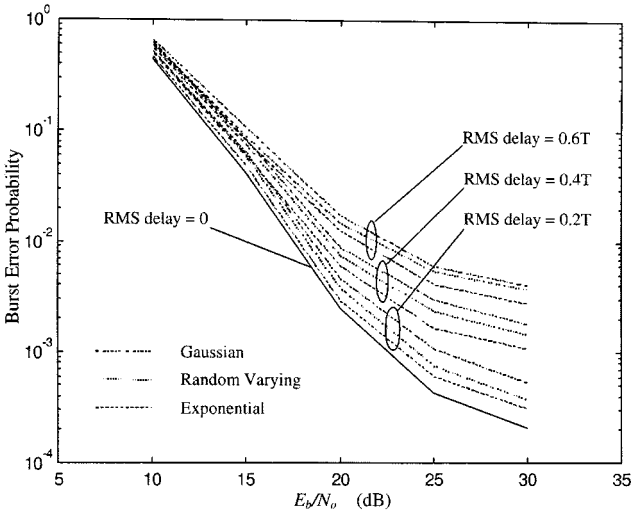

Fig. 7. Burst error probability for channels with different power-delay profiles and the same normalized rms delay spread (three-tap frequency-selective slow fading channal).

A. Effect of Power-Delay Profiles

In this paper, three types of power-delay profiles are considered: one-sided exponential profile, Gaussian profile, and randomly varying profile. The first two types of profiles are given by

$$\sigma_n^2 = \begin{cases} K_e \exp(-\beta_e n), & \text{one-sided exponential} \\ K_g \exp[-\beta_g (n - Q/2)^2], & \text{Gaussian} \end{cases} \tag{15}$$

where K_e, K_g, β_e, and β_g are positive numbers determined by the required rms delay spread and the condition $\sum_n \sigma_n^2 = 1$. As a result, once the value of rms delay spread is given, the average power of each path is fixed. However, for the randomly varying profile, the average power of each path can be varied, so long as the value of rms delay spread remains unchanged. This can be explained by the moving nature of the mobile system. Therefore, for the first two types of profiles, 50 000 randomly generated data bursts were transmitted through the channel with a fixed power-delay profile. For the randomly varying profile, 100 channels with different power-delay profiles were generated for each value of rms delay spread, and 1000 randomly generated data bursts were transmitted through each channel.

Fig. 7 gives the burst error probability versus E_b/N_o for three-tap channels with different types of power delay profiles, as mentioned above, and the same rms delay spread normalized by symbol period. From the simulation results, it can be seen that with the same rms delay spread, the performances for the different types of power-delay profiles are quite close. This implies that the type of channel power-delay profile has negligible effect on the performance of our parallel blind equalization algorithm. Hence, all the simulation results to be presented in the following were obtained for channels with randomly varying power-delay profiles.

B. Flat Fading and Error Floor

In Fig. 7, a burst error probability curve for the case that rms delay spread equals zero is also given for comparison. It can be seen that it serves as a lower bound for all the other burst error probability curves. It should be noted that in this case, the channel becomes a flat fading channel, which has no power-delay profile. Actually, for DQPSK modulation in a quasi-stationary flat fading channel, there should not be any error floor resulting from random FM noise. However, in Fig. 7, it can be seen that an error floor appears to be forming when the value of E_b/N_o becomes large. The reason for this is that the final symbol decision is made according to the output of the receiver y_k, which is the output of a system cascading the channel and equalizer. Since the equalizer tap coefficients are updated symbol by symbol, the impulse response of the cascaded system is no longer quasi-stationary, and therefore error floor appears.

C. Sources of Errors

As explained before, the parallel blind equalization algorithm is not able to eliminate ill-convergence events completely but can reduce their probability. Hence, among all the errors counted, there are contributions from white Gaussian noise, ill convergence, and slow convergence. It is to be noted that slow convergence also contributes to errors because, as mentioned earlier in this section, the equalization run has to be aborted once the number of iterations has reached 250. In Fig. 7, it is observed that for each power-delay profile, the difference of burst error probabilities between different values of rms delay spread is large for high E_b/N_o but becomes smaller as E_b/N_o decreases. This is due to the fact that ill convergence and slow convergence are the dominant factors for the errors that occurred at large values of E_b/N_o. In such situations, the condition of the channel is reflected by the rms delay spread, where a large value gives a channel that is more difficult to equalize. However, at small values of E_b/N_o, white Gaussian noise becomes the dominant factor for the errors and the effect of rms delay spread becomes less significant. As a result, the error performance becomes closer.

D. Simulation Results and Discussions

In Fig. 8, the average burst error probability is plotted against rms delay spread normalized by symbol period with $E_b/N_o = 30$ dB in a three-tap channel ($Q = 2$). The result obtained in [1] is also shown in Fig. 8 for comparison. From the figure, it can be seen that the MCMA-MR proposed here outperforms the equalizer presented in [1] by quite a significant amount. The burst error probability is reduced by more than ten times at small rms delay spread and more than 20 times at large rms delay spread. For a small rms delay spread of less than 0.4 times the symbol period, our blind equalizer without the use of reequalization, as applied in [1], achieves a burst error probability of less than 10^{-3}, which will be suitable for use in voice transmission. Moreover, the result obtained by MCMA-MR using the same initial tap coefficient values to both equalizers is also provided for comparison. It can be seen that by applying different initial tap coefficient values, the burst error probability performance is much better, especially for large rms delay spread. Note that when using the same initial tap coefficient values, due to the presence of the delay before blind equalizer 1, the two equalizers will still have different outputs for mutual referencing purpose.

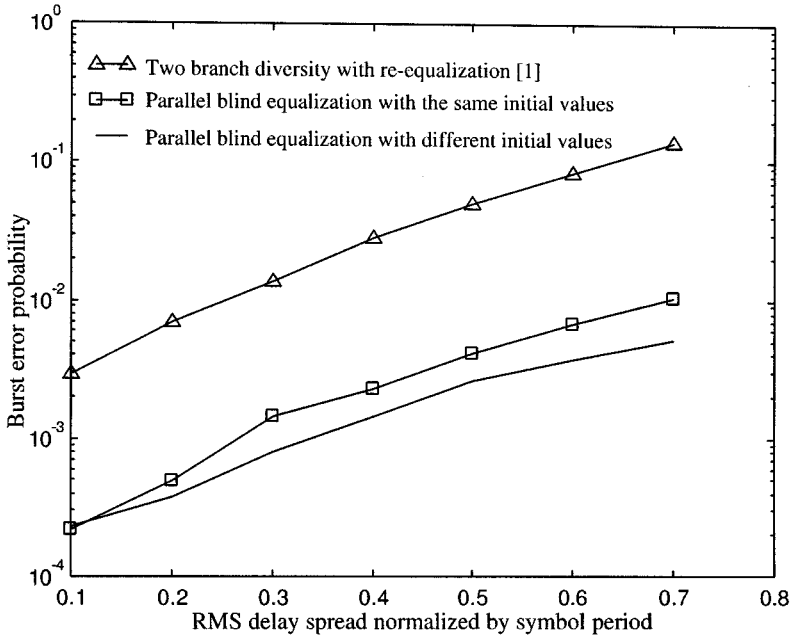

Fig. 8. Comparison of burst error probability with different equalization strategy at $E_b/N_o = 30$ dB.

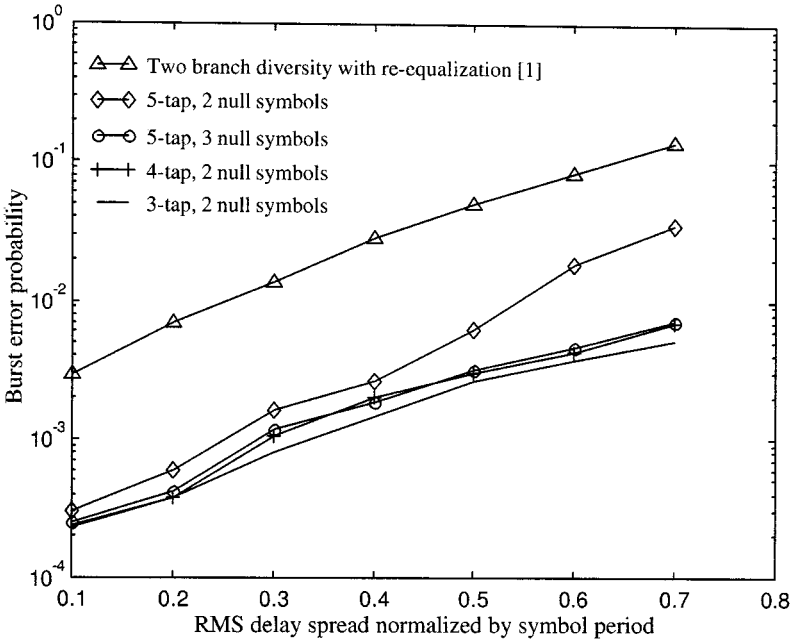

Fig. 9. Comparison of simulation results for different number of channel taps and null symbols at $E_b/N_o = 30$ dB.

The effect of null symbols in the equalization process is illustrated in Fig. 9. All the results were obtained at $E_b/N_o = 30$ dB. From the figure, it can be seen that a four-tap channel with two null symbols has slightly higher burst error probability than that of a three-tap channel with two null symbols. This is because two null symbols are sufficient to remove the interference from the previous burst for a three-tap channel but not for a four-tap, longer delay spread channel. In the case of a five-tap channel, but with only two null symbols, although the equalizer length condition is still satisfied ($L = 5$ is used), the error performance becomes much worse. This is because two null symbols are not sufficient for removing the interburst interference. When we increase the number of null symbols to three, the burst error probability drops considerably, as can be seen from Fig. 9. The burst error probability can reach a similar level as a four-tap channel with two null symbols.

Fig.10 shows the burst error probability versus the maximum number of iterations for a three-tap channel at rms delay spread of 0.6 times symbol period and $E_b/N_o = 20$ dB. As we would expect, the larger the maximum number of iterations, the lower the burst error probability. The burst error probability experiences a significant drop when the number of iterations is approximately larger than 100. The tradeoff for low burst error probability is that longer processing time is required. Therefore, we

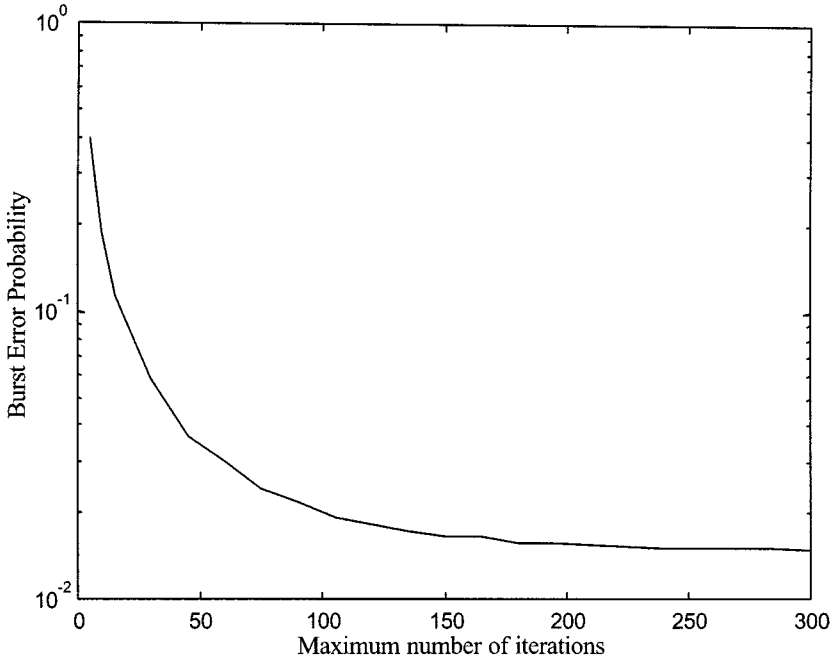

Fig. 10. Burst error probability for different maximum number of iterations at $E_b/N_o = 20$ dB and normalized rms delay spread of 0.6.

took 250 in our simulation as a compromise. It should be noted that the average number of iterations is smaller than the maximum number of iterations since many bursts converge before reaching the maximum number.

V. Conclusion

In this paper, we have presented a q-antenna space diversity receiver and a new blind equalization strategy suitable for a low-delay TDMA system, whose frame is very short. The proposed parallel blind equalization strategy combines MCMA and MR using different initial tap coefficients and appropriate weighting of equalizer outputs for the final symbol decision. We have achieved a significant improvement over the burst error probability performance obtained by Chen *et al.* in [1]. Computer simulation demonstrates that applying different initial coefficient values for parallel blind equalizers indeed gives a better result. Moreover, the length of the null symbols also plays an important role in the equalization process.

References

[1] Y. Chen, J. C.-I. Chuang, and K. B. Letaief, "Blind equalization for short burst TDMA systems in wireless communications," in *Proc. IEEE 47th Vehicular Technology Conf.*, 1997, pp. 535–538.

[2] Z. Ding, R. A. Kennedy, B. D. O. Anderson, and C. R. Johnson, "Ill convergence of Godard blind equalization in data communication systems," *IEEE Trans. Commun.*, vol. 39, pp. 1313–1327, Sept. 1991.

[3] D. N. Godard, "Self-recovering equalization and carrier tracking in two-dimensional data communications systems," *IEEE Trans. Commun.*, vol. COM-28, pp. 1867–1875, Nov. 1980.

[4] Y. Li and Z. Ding, "Global convergence of fractionally spaced Godard (CMA) adaptive equalizers," *IEEE Trans. Signal Processing*, vol. 44, pp. 818–826, Apr. 1996.

[5] A. Touzni and I. Fijalkow, "Channel robust blind fractionally spaced equalization," in *Proc. IEEE SPAWC-97*, 1997, pp. 33–37.

[6] D. Gesbert, P. Duhamel, and S. Mayrargue, "On-line blind multichannel equalization based on mutually referenced filters," *IEEE Trans. Signal Processing*, vol. 45, pp. 2307–2317, Sept. 1997.

[7] K. N. Oh and Y. O. Chin, "Modified constant modulus algorithm: Blind equalization and carrier phase recovery algorithm," in *Proc. IEEE ICC*, 1995, pp. 498–501.

[8] I. Fijalkow, A. Touzni, and J. R. Treichler, "Fractionally spaced equalization using CMA: Robustness to channel noise and lack of disparity," *IEEE Trans. Signal Processing*, vol. 45, pp. 56–66, Jan. 1997.

[9] J. G. Proakis, *Digital Communications*, 3rd ed. New York: McGraw-Hill, 1995.

[10] S. Haykin, *Adaptive Filter Theory*, 3rd ed. Englewood Cliffs, NJ: Prentice-Hall, 1996.

Hongyi Qian was born in Shanghai, China, in 1977. He received the B.Eng. and M.Eng. degrees in electrical engineering from the National University of Singapore in 1999 and 2000, respectively.

Since 2000, he has been a System Engineer with the Semiconductor Product Sector, Motorola Electronics Pte Ltd., Singapore. He has been involved in the design and development of the Bluetooth system. His research interests include digital wireless communications, signal processing, and channel coding.

Tjeng Thiang Tjhung (SM'84) received the B.Eng. and M.Eng. degrees in electrical engineering from Carleton University, Ottawa, ON, Canada, in 1963 and 1965, respectively, and the Ph.D. degree from Queen's University, Kingston, ON, in 1969.

From 1963 to 1968, he was a Consultant with Acres-Inter-Tel Ltd., Ottawa, where his work was concerned with FSK systems for secure radio communication. In 1969, he joined the National University of Singapore, where he was a Professor in the Department of Electrical and Computer Engineering until March 2000. He is now with the Centre for Wireless Communications, National University of Singapore, as a Distinguished Member of Technical Staff in their Communications Division. His present research interests are in bandwidth-efficient digital modulation techniques for mobile radio and in multicarrier and code-division multiple-access communication systems. From 1977 to 1983, he was a Consultant to Singapore Telecom on the planning and implementation of their optical fiber wide-band network.

Dr. Tjhung is a Fellow of IES Singapore and a member of IEICE Japan and the Association of Professional Engineers of Singapore.

Ping He received the B.Sc. and M.Eng. degrees from the University of Electronic and Science Technology of China, Chendu, in 1983 and 1986, respectively, and the Ph.D. degree from Xidian University, Xian, China, in 1994.

From 1986 to 1996, he was with the Department of Electrical and Communications Engineering, Xidian University, where his work was concerned with HF MODEM and its key techniques, such as adaptive equalization, coded modulation/demodulation, and encoding/decoding. Since 1996, he has been with the Centre for Wireless Communications, National University of Singapore, Singapore, where he is currently a Senior Member of Technical Staff of the Communication System and Signal Processing Group. His current research interests are in mobile radio digital communications, such as multiuser detection of CDMA, OFDM systems in wireless LAN or Hiperlan II, and synchronization and equalization of communications systems.

Fumiyuki Adachi (M'79–SM'90) received the B.S. and Dr. Eng. degrees in electrical engineering from Tohoku University, Sendai, Japan, in 1973 and 1984, respectively.

In 1973, he joined the Electrical Communications Laboratories, Nippon Telegraph & Telephone Corporation (now NTT), where he conducted various types of research related to digital cellular mobile communications. From 1992 to 1999, he was with NTT Mobile Communications Network, Inc. (now NTT DoCoMo, Inc.), where he led a research group on wideband/broadband CDMA wireless access for IMT-2000 and beyond. Since January 2000, he has been with Tohoku University, Sendai, where he is a Professor of electrical and communication engineering at the Graduate School of Engineering. His research interests are in OFDM, CDMA, and TDMA wireless access techniques; transmit/receive antenna diversity; adaptive antenna arrays; bandwidth-efficient digital modulation; and channel coding, with particular application to broadband mobile wireless communications systems. From October 1984 to September 1985, he was a United Kingdom SERC Visiting Research Fellow in the Department of Electrical Engineering and Electronics, Liverpool University. From April 1997 to March 2000, he was a Visiting Professor at the Nara Institute of Science and Technology, Japan.

Dr. Adachi is a member of the Institute of Electronics, Information and Communication Engineers of Japan (IEICE) of Japan. He was a Guest Editor of the IEEE JOURNAL ON SELECTED TOPICS IN COMMUNICATIONS for a special issue on Broadband Wireless Techniques (October 1999) and a special issue on Wideband CDMA I (August 2000). He was a Corecipient of the IEEE TRANSACTIONS ON VEHICULAR TECHNOLOGY Best Paper of the Year Award in 1980 and 1990. He received the Avant Garde award 2000. He was a Corecipient of the *IEICE Transactions* Best Paper of the Year Award in 1996 and 1998.